# On the Accuracy of Localization Systems Using Wideband Antenna Arrays

Yuan Shen, *Student Member, IEEE,* and Moe Z. Win, *Fellow, IEEE*

***Abstract*—Accurate positional information is essential for many applications in wireless networks. Time-of-arrival (TOA) and angle-of-arrival (AOA) are the two most commonly used signal metrics for localizing nodes with unknown positions. In this paper, we consider a wireless network in which each node is equipped with a wideband antenna array capable of performing both TOA and AOA measurements. Since both the position and orientation of the agent are of interest, we propose a localization framework that jointly estimates these two parameters. The notion of equivalent Fisher information is applied to derive the squared error bounds for the position and orientation. Since our analysis starts from the received waveforms rather than directly from the signal metrics, these bounds characterize the fundamental limits of the position and orientation accuracy. Surprisingly, our result reveals that AOA measurements obtained by wideband antenna arrays do not further improve position accuracy beyond that provided by TOA measurements.**

***Index Terms*—Localization, wideband antenna array, equivalent Fisher information (EFI), Cramèr-Rao bound (CRB), squared position error bound (SPEB), squared orientation error bound (SOEB).**

## I. Introduction

LOCALIZATION in an absolute frame through Global Positioning Systems (GPS) has found applications in many different fields [1]. However, due to the inability of GPS signals to penetrate most obstacles, the effectiveness of GPS is limited in harsh environments, such as in buildings, in urban canyons, under tree canopies, and in caves [2]. To address this problem, wireless networks employing wideband transmission techniques have recently been introduced for localization in GPS-denied environments [2]–[15]. In these networks, each node is equipped with a wide bandwidth transceiver. Wide bandwidth or ultrawide bandwidth (UWB) signals are inherently well-suited for localization: in addition to communication, these signals can provide precise range measurements due to their fine delay resolution and robustness in cluttered environments [14], [16]–[23].

We consider a wireless network consisting of anchors and agents, in which each node is equipped with a wideband antenna array. Anchors are nodes with known positions and orientations (for example, by GPS or system design). Agents are nodes with unknown positions and/or orientations, and they attempt to determine this information based on the waveforms received from neighboring anchors. Thus, localization in this paper refers to determining both the *position* and *orientation* of the agent.

The angle at which a signal arrives at the agent, known as AOA, provides information about the agent's position and orientation relative to the anchor. AOA can be estimated using an array of antennas, based on the received waveforms at each antenna.[1] The use of the AOA metric for localization has been investigated, and many hybrid systems have been proposed. These include hybrid TOA/AOA systems [29]–[31], and hybrid time-difference-of-arrival (TDOA)/AOA systems [32]. However, some of these studies employ narrowband signal models, and others are restricted to far-field scenarios or use far-field assumptions. A general framework to analyze localization systems using wideband antenna arrays in various scenarios needs to be developed.

Performance bounds for wideband localization using a single antenna have been derived in [4]–[7], [9]. In this paper, we investigate the accuracy of localization systems that employ wideband antenna arrays. Our analysis starts from the received waveforms rather than directly from TOA and AOA metrics, and hence the results characterize the *fundamental limits* of localization accuracy. The main contributions of this paper are as follows:

- We derive the fundamental limits of localization accuracy for wireless networks employing *wideband antenna arrays*, in terms of performance measures called the squared position error bound (SPEB) and squared orientation error bound (SOEB).
- We apply the notion of the equivalent Fisher information (EFI) [6], [7], which enables us to succinctly derive the SPEB and SOEB. This methodology also provides insights into the essence of the localization problem by unifying the *localization information* from anchors in a canonical form.
- We prove that the AOA measurements by antenna arrays do not further improve the position accuracy beyond that provided by TOA measurements, since the AOA is

Paper approved by X. Wang, the Editor for Multiuser Detection and Equalization of the IEEE Communications Society. Manuscript submitted March 29, 2008; revised November 15, 2008.

This paper was presented in part at the IEEE International Conference on Ultra-Wideband, Singapore, Sept. 2007. This research was supported, in part, by the National Science Foundation under Grants ECCS-0636519 and ECCS-0901034, the Office of Naval Research Presidential Early Career Award for Scientists and Engineers (PECASE) N00014-09-1-0435, and MIT Institute for Soldier Nanotechnologies.

The authors are with the Laboratory for Information and Decision Systems (LIDS), Massachusetts Institute of Technology, Room 32-D674, 77 Massachusetts Avenue, Cambridge, MA 02139 USA (e-mail: {shenyuan, moewin}@mit.edu).

Digital Object Identifier 10.1109/TCOMM.2010.01.080141

[1]There are two ways to obtain the AOA: the first is through measurement by a directional antenna, and the second is indirectly through TOA measurements using an antenna array [24]–[27]. Wideband directional antennas that satisfy size and cost requirements are difficult to implement, since they are required to work across a large bandwidth [28]. As such, antenna arrays are more commonly used when angle measurement for wide bandwidth signals is necessary.

obtained through the TOAs at the antennas in the array.
- We show that exploiting the geometric relationship inherent in multipath propagation does not further improve the localization accuracy by antenna arrays.

We also apply the SOEB analysis to AOA estimation using wideband antenna arrays and compare the performance of two specific array geometries, i.e., the uniform linear array (ULA) and uniform circular array (UCA).

The rest of the paper is organized as follows. Section II presents a wideband antenna array model for localization and puts forth the concepts of the SPEB and SOEB in terms of the Fisher information. The SPEB and SOEB are derived using the notion of EFI in Section III. Discussion and examples are given in Section IV. Some numerical illustrations are provided in Section V, and conclusions are drawn in the last section.

*Notations:* The notation $\mathbb{E}_{\mathbf{z}}\{\cdot\}$ is the expectation operator with respect to the random vector $\mathbf{z}$; $\mathbf{A} \succ \mathbf{B}$ and $\mathbf{A} \succeq \mathbf{B}$ denote that the matrix $\mathbf{A}-\mathbf{B}$ is positive definite and positive semi-definite, respectively; $\mathrm{tr}\{\cdot\}$ denotes the trace of a square matrix; $[\,\cdot\,]_{n\times n}$ denotes the upper left $n \times n$ submatrix of its argument; $[\,\cdot\,]_{n,m}$ denotes the element at the $n$th row and $m$th column of its argument; $\|\cdot\|$ denotes the Euclidean distance; and the superscript $[\,\cdot\,]^{\mathrm{T}}$ denotes the transpose of its argument. We denote by $f(\mathbf{x})$ the probability density function (PDF) $f_{\mathbf{X}}(\mathbf{x})$ of the random vector $\mathbf{X}$ unless specified otherwise, and we use the following function for the Fisher information matrix (FIM):

$$\mathbf{F}_{\mathbf{z}}(\mathbf{w}\,;\mathbf{x},\mathbf{y}) \triangleq \mathbb{E}_{\mathbf{z}}\left\{\left[\frac{\partial}{\partial \mathbf{x}}\ln f(\mathbf{w})\right]\left[\frac{\partial}{\partial \mathbf{y}}\ln f(\mathbf{w})\right]^{\mathrm{T}}\right\}. \quad (1)$$

## II. System Model and Mathematical Preliminaries

In this section, we first present a model for location-aware networks employing wideband antenna arrays together with an associated channel propagation model. We then put forth performance measures called the squared position and orientation error bounds (SPEB/SOEB) in terms of the Fisher information matrix.

### A. Network Model

Consider a network consisting of $N_{\mathrm{b}}$ anchors and multiple agents with a fixed topology. Each anchor is equipped with a single antenna,[2] and each agent is equipped with an array of $N_{\mathrm{a}}$ antennas, which can obtain both TOA and AOA measurements with respect to their neighboring anchors. Radio signals traveling from anchors to agents are subject to multipath propagation. The agents estimate their positions and orientations based on the received waveforms. Without loss of generality, we focus on one agent in the network, since agents estimate their positions and orientations independently.

Let $\mathcal{N}_{\mathrm{b}} = \{1, 2, \ldots, N_{\mathrm{b}}\}$ be the set of all anchors with known positions $\mathbf{p}_k \triangleq [\,x_k \;\; y_k\,]^{\mathrm{T}}$ ($k \in \mathcal{N}_{\mathrm{b}}$). Let $\mathcal{N}_{\mathrm{a}} = \{1, 2, \ldots, N_{\mathrm{a}}\}$ be the set of antennas, and $\tilde{\mathbf{p}}_n \triangleq [\,\tilde{x}_n \;\; \tilde{y}_n\,]^{\mathrm{T}}$ (with $n \in \mathcal{N}_{\mathrm{a}}$) denotes the position of the agent's $n$th antenna, which needs to be estimated.[3] Let $\phi_{n,k}$ denote the angle from anchor $k$ to the $n$th antenna, and $\mathbf{q}_{n,k} \triangleq [\,\cos\phi_{n,k} \quad \sin\phi_{n,k}\,]^{\mathrm{T}}$ denote the corresponding normal vector.

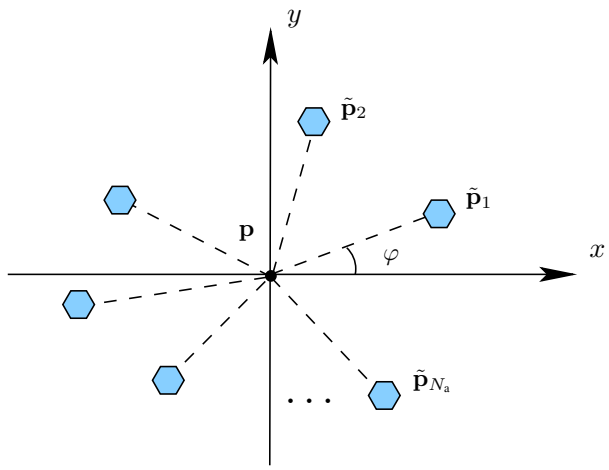


Fig. 1. An antenna array with arbitrary geometry is described by the reference point $\mathbf{p}$, the orientation $\varphi$, and the relative positions of the antennas.

Note that the relative positions of the antennas in the array are usually known. Hence if we denote $\mathbf{p} = [\,x \;\; y\,]^{\mathrm{T}}$ as a reference point and $\varphi$ as the orientation of the array,[4] then the position of the $n$th antenna in the array can be represented as

$$\tilde{\mathbf{p}}_n = \mathbf{p} + \begin{bmatrix} \Delta x_n(\mathbf{p},\varphi) \\ \Delta y_n(\mathbf{p},\varphi) \end{bmatrix}, \qquad n \in \mathcal{N}_{\mathrm{a}}\,,$$

where $\Delta x_n(\mathbf{p},\varphi)$ and $\Delta y_n(\mathbf{p},\varphi)$ denote the relative distance in $x$ and $y$ direction from the reference point $\mathbf{p}$ to the $n$th antenna. The reference point can be arbitrary, but one natural choice is the array center, which is defined as the value $\mathbf{p}_0$ satisfying

$$\sum_{n\in\mathcal{N}_{\mathrm{a}}} \Delta x_n(\mathbf{p}_0,\varphi) = 0 \quad \text{and} \quad \sum_{n\in\mathcal{N}_{\mathrm{a}}} \Delta y_n(\mathbf{p}_0,\varphi) = 0\,.$$

As mentioned before, localization in this paper involves determining both the position and the orientation of the agent. In some scenarios, either the position or the orientation of the agent may be known, and then we have two special localization problems, *position-aware* localization and *orientation-aware* localization, respectively. Correspondingly, from the perspective of Bayesian estimation, $\mathbf{p}$ and $\varphi$ can be thought of as random parameters with infinite a priori Fisher information for position-aware and orientation-aware localization, respectively [7].

### B. Channel Model

The received waveform from anchor $k$ at the $n$th antenna of the agent in passband can be written as

$$r_{n,k}(t) = \sum_{l=1}^{L_{n,k}} \alpha_{n,k}^{(l)}\, s\left(t-\tau_{n,k}^{(l)}\right) + z_{n,k}(t)\,, \quad t \in [\,0, T_{\mathrm{ob}})\,, \quad (2)$$

[2]The case in which an anchor is equipped with multiple antennas will be addressed in Section IV. An anchor with multiple antennas can be thought of as multiple anchors, each of which has a single antenna.

[3]Our discussion is focused on two-dimensional localization, and its results can be easily extended to three-dimensional cases.

[4]Note from geometry that the orientation $\varphi$ is independent of the specific reference points.

where $s(t)$ is a known wideband waveform, $\alpha_{n,k}^{(l)}$ and $\tau_{n,k}^{(l)}$ are the amplitude and delay, respectively, of the $l$th path, $L_{n,k}$ is the number of multipath components (MPCs), $z_{n,k}(t)$ represents the observation noise modeled as additive white Gaussian processes with two-side power spectral density $N_0/2$, and $[0, T_{\text{ob}})$ is the observation interval. The relationship between the $n$th antenna's position and the delay of the $l$th path is given by

$$\tau_{n,k}^{(l)} = \frac{1}{c}\left[\|\mathbf{p}_k - \tilde{\mathbf{p}}_n\| + b_{n,k}^{(l)}\right], \tag{3}$$

where $c$ is the propagation speed of the signal, and $b_{n,k}^{(l)} \geq 0$ is a range bias. The range bias $b_{n,k}^{(1)} = 0$ for line of sight (LOS) propagation, whereas $b_{n,k}^{(l)} > 0$ for non-line of sight (NLOS) propagation.

Our analysis is based on the received waveforms given by (2), and hence the parameters to be estimated include the position of the reference point, the array orientation, and the nuisance multipath parameters, i.e.,

$$\boldsymbol{\theta} = \begin{bmatrix} \mathbf{p}^{\mathrm{T}} & \varphi & \boldsymbol{\kappa}^{\mathrm{T}} \end{bmatrix}^{\mathrm{T}}, \tag{4}$$

where $\boldsymbol{\kappa}$ is the vector consisting of all the multipath parameters associated with the received waveforms, i.e., $b_{n,k}^{(l)}$ and $\alpha_{n,k}^{(l)}$ for $n \in \mathcal{N}_{\text{a}}$, $k \in \mathcal{N}_{\text{b}}$, and $l = 1, 2, ..., L_{n,k}$.

### C. Bounds for Squared Position and Orientation Errors

Let $\hat{\boldsymbol{\theta}}$ denote an estimate of the parameter vector $\boldsymbol{\theta}$ based on the observation vector

$$\mathbf{r} = \begin{bmatrix} \mathbf{r}_1^{\mathrm{T}} & \mathbf{r}_2^{\mathrm{T}} & \cdots & \mathbf{r}_{N_{\text{a}}}^{\mathrm{T}} \end{bmatrix}^{\mathrm{T}},$$

where $\mathbf{r}_n = \begin{bmatrix} \mathbf{r}_{n,1}^{\mathrm{T}} & \mathbf{r}_{n,2}^{\mathrm{T}} & \cdots & \mathbf{r}_{n,N_{\text{b}}}^{\mathrm{T}} \end{bmatrix}^{\mathrm{T}}$ in which the elements of $\mathbf{r}_{n,k}$ can be obtained from the Karhunen-Loève expansion of $r_{n,k}(t)$ [33], [34]. The mean squared error (MSE) matrix of $\hat{\boldsymbol{\theta}}$ satisfies the information inequality [33], [35]

$$\mathbb{E}_{\mathbf{r},\boldsymbol{\theta}}\left\{(\hat{\boldsymbol{\theta}} - \boldsymbol{\theta})(\hat{\boldsymbol{\theta}} - \boldsymbol{\theta})^{\mathrm{T}}\right\} \succeq \mathbf{J}_{\boldsymbol{\theta}}^{-1}, \tag{5}$$

where $\mathbf{J}_{\boldsymbol{\theta}}$ is the FIM for the parameter vector $\boldsymbol{\theta}$.[5]

Equation (5) implies that the MSE of the position estimate $\hat{\mathbf{p}}$ and that of the orientation estimate $\hat{\varphi}$ are bounded below by

$$\mathcal{P}(\mathbf{p}) \triangleq \mathrm{tr}\left\{\left[\mathbf{J}_{\boldsymbol{\theta}}^{-1}\right]_{2\times 2}\right\}, \tag{6}$$

and

$$\mathcal{P}(\varphi) \triangleq \left[\mathbf{J}_{\boldsymbol{\theta}}^{-1}\right]_{3,3}, \tag{7}$$

respectively. In the following, we refer to $\mathcal{P}(\mathbf{p})$ and $\mathcal{P}(\varphi)$ as the squared position error bound (SPEB) and the squared orientation error bound (SOEB), respectively [6].

[5]More precisely, $\mathbf{J}_{\boldsymbol{\theta}}$ is called the Bayesian information matrix if the parameter vector $\boldsymbol{\theta}$ is random, and the corresponding lower bound is called the Bayesian Cramèr-Rao bound or the hybrid Bayesian Cramèr-Rao bound, respectively, if all or some parameters in $\boldsymbol{\theta}$ are random. In this paper, we do not distinguish these names.

### D. Fisher Information Matrix

We first consider the case in which a priori knowledge of the channel parameters, the agent's position, and the agent's orientation is not available. The results will be extended to cases where a priori knowledge is available in Section IV.

Since the observation noise in the received waveforms $r_{n,k}(t)$ from different $n$'s and $k$'s are independent, the likelihood function of the observation $\mathbf{r}$ conditioned on $\boldsymbol{\theta}$ can be written as

$$f(\mathbf{r}|\boldsymbol{\theta}) = \prod_{n\in\mathcal{N}_{\text{a}}}\prod_{k\in\mathcal{N}_{\text{b}}} f(\mathbf{r}_{n,k}|\boldsymbol{\theta}),$$

where each term in the above factor is given by [33]

$$f(\mathbf{r}_{n,k}|\boldsymbol{\theta}) \propto \exp\left\{\frac{2}{N_0}\int_0^{T_{\text{ob}}} r_{n,k}(t)\sum_{l=1}^{L_{n,k}}\alpha_{n,k}^{(l)}\, s(t-\tau_{n,k}^{(l)})\, dt - \frac{1}{N_0}\int_0^{T_{\text{ob}}}\left[\sum_{l=1}^{L_{n,k}}\alpha_{n,k}^{(l)}\, s(t-\tau_{n,k}^{(l)})\right]^2 dt\right\}. \tag{8}$$

We then have the FIM for the parameter vector $\boldsymbol{\theta}$ as follows

$$\mathbf{J}_{\boldsymbol{\theta}} \triangleq \mathbf{F}_{\mathbf{r}}(\mathbf{r}|\boldsymbol{\theta}\,;\boldsymbol{\theta},\boldsymbol{\theta}), \tag{9}$$

where the right-hand side is defined in (1) except that $\mathbf{w}$ is replaced by $\mathbf{r}|\boldsymbol{\theta}$.

## III. Evaluation of FIM and SPEB/SOEB

The SPEB and SOEB can be evaluated by taking the inverse of the FIM $\mathbf{J}_{\boldsymbol{\theta}}$ in (9). However, $\mathbf{J}_{\boldsymbol{\theta}}$ is a matrix of very high dimension, while only $[\mathbf{J}_{\boldsymbol{\theta}}^{-1}]_{2\times 2}$ and $[\mathbf{J}_{\boldsymbol{\theta}}^{-1}]_{3,3}$ (or equivalently $[\mathbf{J}_{\boldsymbol{\theta}}^{-1}]_{3\times 3}$) are of interest. To circumvent direction matrix inversion and gain insights into the problem, we apply the notion of EFI introduced in [4], [6], which retains all the necessary information to obtain the information inequality for a subset of parameters.

### A. Equivalent Fisher Information Matrix for SPEB and SOEB

In this subsection, we derive the equivalent Fisher information matrix (EFIM) for the position and the EFI for the orientation.

Let $\boldsymbol{\eta}_{n,k} \triangleq \begin{bmatrix} \tau_{n,k}^{(1)} & \tilde{\alpha}_{n,k}^{(1)} & \tau_{n,k}^{(2)} & \tilde{\alpha}_{n,k}^{(2)} & \cdots & \tau_{n,k}^{(L_{n,k})} & \tilde{\alpha}_{n,k}^{(L_{n,k})} \end{bmatrix}^{\mathrm{T}}$, where $\tilde{\alpha}_{n,k}^{(l)} \triangleq \alpha_{n,k}^{(l)}/c$. After some algebra, the FIM can be derived as (10), shown at the bottom of the next page, where[6]

$$\mathbf{G}_n = \begin{bmatrix} \mathbf{q}_{n,1}\mathbf{l}_{n,1}^{\mathrm{T}} & \mathbf{q}_{n,2}\mathbf{l}_{n,2}^{\mathrm{T}} & \cdots & \mathbf{q}_{n,N_{\text{b}}}\mathbf{l}_{n,N_{\text{b}}}^{\mathrm{T}} \end{bmatrix},$$
$$\mathbf{h}_n = \begin{bmatrix} h_{n,1}\mathbf{l}_{n,1}^{\mathrm{T}} & h_{n,2}\mathbf{l}_{n,2}^{\mathrm{T}} & \cdots & h_{n,N_{\text{b}}}\mathbf{l}_{n,N_{\text{b}}}^{\mathrm{T}} \end{bmatrix},$$

with

$$h_{n,k} = \frac{d}{d\varphi}\Delta x_n(\mathbf{p},\varphi)\cos\phi_{n,k} + \frac{d}{d\varphi}\Delta y_n(\mathbf{p},\varphi)\sin\phi_{n,k},$$
$$\mathbf{l}_{n,k} = \underbrace{\begin{bmatrix} 1 & 0 & 1 & 0 & \cdots & 1 & 0 \end{bmatrix}^{\mathrm{T}}}_{2L_{n,k}\ \text{components}};$$

and

$$\boldsymbol{\Lambda}_n = \mathrm{diag}\left\{\boldsymbol{\Psi}_{n,1}, \boldsymbol{\Psi}_{n,2}, \ldots, \boldsymbol{\Psi}_{n,N_{\text{b}}}\right\},$$

[6]Without confusion, unspecified elements are 0 in this paper.

with $\mathbf{\Psi}_{n,k} \triangleq \mathbf{F}_{\mathbf{r}}(\mathbf{r}|\boldsymbol{\theta}\,; \boldsymbol{\eta}_{n,k}, \boldsymbol{\eta}_{n,k})$. In particular, the diagonal elements in $\mathbf{\Psi}_{n,k}$ are

$$\mathbf{F}_{\mathbf{r}}(\mathbf{r}|\boldsymbol{\theta}\,; \tau_{n,k}^{(l)}, \tau_{n,k}^{(l)}) = 8\pi^2\beta^2\,\mathsf{SNR}_{n,k}^{(l)}\,, \tag{11}$$

where

$$\beta = \left(\frac{\int_{-\infty}^{+\infty} f^2\,|S(f)|^2 df}{\int_{-\infty}^{+\infty} |S(f)|^2 df}\right)^{1/2}, \tag{12}$$

and

$$\mathsf{SNR}_{n,k}^{(l)} = \frac{{\alpha_{n,k}^{(l)}}^2 \int_{-\infty}^{+\infty} |S(f)|^2 df}{N_0}\,.$$

In the above, $\beta$ is known as the effective bandwidth [33], and $S(f)$ is the Fourier transform of $s(t)$.

By applying the notion of EFI to (10), we can derive the $3\times 3$ EFIM $\mathbf{J}_{\mathrm{e}}(\mathbf{p})$, after some algebra, as[7]

$$\mathbf{J}_{\mathrm{e}}(\mathbf{p},\varphi) = \sum_{n\in\mathcal{N}_{\mathrm{a}}}\sum_{k\in\mathcal{N}_{\mathrm{b}}} \begin{bmatrix} \lambda_{n,k}\,\mathbf{q}_{n,k}\,\mathbf{q}_{n,k}^{\mathrm{T}} & \lambda_{n,k}h_{n,k}\,\mathbf{q}_{n,k} \\ \lambda_{n,k}h_{n,k}\,\mathbf{q}_{n,k}^{\mathrm{T}} & \lambda_{n,k}h_{n,k}^2 \end{bmatrix}, \tag{13}$$

where $\lambda_{n,k}$ is called the ranging information intensity (RII)[8] from anchor $k$ to the $n$th antenna given by (14), shown at the bottom of this page, in which $\mathbf{D}_{n,k} = \begin{bmatrix}\mathbf{0} & \mathbf{I}_{2L_{n,k}-1}\end{bmatrix}$. Note that in the case of LOS signals, we eliminate $b_{n,k}^{(1)}$ from $\boldsymbol{\kappa}_{n,k}$ and the corresponding rows and columns from $\mathbf{J}_{\boldsymbol{\theta}}$ since they are known to be 0.

Therefore, the EFIM for the position and the EFI for the orientation, using an $N_{\mathrm{a}}$-antenna array, can be obtained from (13) as

$$\mathbf{J}_{\mathrm{e}}(\mathbf{p}) = \sum_{n\in\mathcal{N}_{\mathrm{a}}}\sum_{k\in\mathcal{N}_{\mathrm{b}}} \lambda_{n,k}\,\mathbf{q}_{n,k}\,\mathbf{q}_{n,k}^{\mathrm{T}} - \frac{1}{\sum_{n\in\mathcal{N}_{\mathrm{a}}}\sum_{k\in\mathcal{N}_{\mathrm{b}}}\lambda_{n,k}h_{n,k}^2}\,\mathbf{q}\,\mathbf{q}^{\mathrm{T}}, \tag{15}$$

and

$$J_{\mathrm{e}}(\varphi) = \sum_{n\in\mathcal{N}_{\mathrm{a}}}\sum_{k\in\mathcal{N}_{\mathrm{b}}} \lambda_{n,k}h_{n,k}^2 - \mathbf{q}^{\mathrm{T}}\left[\sum_{n\in\mathcal{N}_{\mathrm{a}}}\sum_{k\in\mathcal{N}_{\mathrm{b}}}\lambda_{n,k}\,\mathbf{q}_{n,k}\,\mathbf{q}_{n,k}^{\mathrm{T}}\right]^{-1}\mathbf{q}\,, \tag{16}$$

where

$$\mathbf{q} = \sum_{n\in\mathcal{N}_{\mathrm{a}}}\sum_{k\in\mathcal{N}_{\mathrm{b}}}\lambda_{n,k}\,h_{n,k}\,\mathbf{q}_{n,k}\,.$$

Note that the angle $\varphi$ is known in the orientation-aware case, and hence excluded from the parameter vector $\boldsymbol{\theta}$ in (4). Consequently, the components corresponding to $\varphi$ are eliminated from the FIMs in (10) and (13), and the EFIM for the position in (15) becomes

$$\mathbf{J}_{\mathrm{e}}(\mathbf{p}) = \sum_{n\in\mathcal{N}_{\mathrm{a}}}\sum_{k\in\mathcal{N}_{\mathrm{b}}}\lambda_{n,k}\,\mathbf{q}_{n,k}\,\mathbf{q}_{n,k}^{\mathrm{T}}\,. \tag{17}$$

Similarly, in the position-aware case, $\mathbf{p}$ is eliminated from $\boldsymbol{\theta}$, and (16) becomes

$$J_{\mathrm{e}}(\varphi) = \sum_{n\in\mathcal{N}_{\mathrm{a}}}\sum_{k\in\mathcal{N}_{\mathrm{b}}}\lambda_{n,k}\,h_{n,k}^2\,.$$

### *B. Remarks on the EFIM*

Since $\mathbf{q}\,\mathbf{q}^{\mathrm{T}}$ in (15) is a positive semi-definite $2\times 2$ matrix and $\sum_{n\in\mathcal{N}_{\mathrm{a}}}\sum_{k\in\mathcal{N}_{\mathrm{b}}}\lambda_{n,k}\,h_{n,k}^2 > 0$, we have[9]

$$\mathbf{J}_{\mathrm{e}}(\mathbf{p}) \preceq \sum_{n\in\mathcal{N}_{\mathrm{a}}}\sum_{k\in\mathcal{N}_{\mathrm{b}}}\lambda_{n,k}\,\mathbf{q}_{n,k}\,\mathbf{q}_{n,k}^{\mathrm{T}}\,. \tag{18}$$

Note that the right-hand side of (18) is the sum of localization information obtained from individual antennas [6]. This implies that the EFIM for the position, using antenna arrays, is bounded above by the sum of all EFIMs corresponding to individual antennas. The inequality of (18) is due to the uncertainty associated with the unknown orientation, and the equality is achieved for the cases of $\mathbf{q} = 0$ or orientation-aware localization (c.f. (17)).

We have shown in [6] that in orientation-unaware localization there exists a unique reference point $\mathbf{p}^*$, called *orientation center*, such that the equality in (18) is achieved, and the SPEB of any other reference point is strictly larger than that of $\mathbf{p}^*$. In general, $\mathbf{p}^*$ depends on the topology of the anchors and

[7]The notation $\mathbf{J}_{\mathrm{e}}(\boldsymbol{\theta}_1)$ denotes the EFIM for the parameter vector $\boldsymbol{\theta}_1 \subseteq \boldsymbol{\theta}$. Note that $\mathbf{J}_{\mathrm{e}}(\boldsymbol{\theta}_1)$ does not depend on the value of $\boldsymbol{\theta}_1$ for a random parameter vector $\boldsymbol{\theta}_1$, whereas it may be a function of $\boldsymbol{\theta}_1$ for a deterministic parameter vector $\boldsymbol{\theta}_1$.

[8]The RII is determined by the SNR of the received waveform, the effective bandwidth of the pulse, the multipath propagation condition, and the a priori channel knowledge if available [6].

[9]For notational convenience, we suppress the dependence of $h_{n,k}$, $\lambda_{n,k}$, and $\mathbf{q}$ on the reference position $\mathbf{p}$ throughout the paper.

$$\mathbf{J}_{\boldsymbol{\theta}} = \frac{1}{c^2}\begin{bmatrix} \sum_{n\in\mathcal{N}_{\mathrm{a}}}\mathbf{G}_n\mathbf{\Lambda}_n\mathbf{G}_n^{\mathrm{T}} & \sum_{n\in\mathcal{N}_{\mathrm{a}}}\mathbf{G}_n\mathbf{\Lambda}_n\mathbf{h}_n^{\mathrm{T}} & \mathbf{G}_1\mathbf{\Lambda}_1 & \cdots & \mathbf{G}_{N_{\mathrm{a}}}\mathbf{\Lambda}_{N_{\mathrm{a}}} \\ \sum_{n\in\mathcal{N}_{\mathrm{a}}}\mathbf{h}_n\mathbf{\Lambda}_n\mathbf{G}_n^{\mathrm{T}} & \sum_{n\in\mathcal{N}_{\mathrm{a}}}\mathbf{h}_n\mathbf{\Lambda}_n\mathbf{h}_n^{\mathrm{T}} & \mathbf{h}_1\mathbf{\Lambda}_1 & \cdots & \mathbf{h}_{N_{\mathrm{a}}}\mathbf{\Lambda}_{N_{\mathrm{a}}} \\ \mathbf{\Lambda}_1\mathbf{G}_1^{\mathrm{T}} & \mathbf{\Lambda}_1\mathbf{h}_1^{\mathrm{T}} & \mathbf{\Lambda}_1 & & \\ \vdots & \vdots & & \ddots & \\ \mathbf{\Lambda}_{N_{\mathrm{a}}}\mathbf{G}_{N_{\mathrm{a}}}^{\mathrm{T}} & \mathbf{\Lambda}_{N_{\mathrm{a}}}\mathbf{h}_{N_{\mathrm{a}}}^{\mathrm{T}} & & & \mathbf{\Lambda}_{N_{\mathrm{a}}} \end{bmatrix} \tag{10}$$

$$\lambda_{n,k} = \begin{cases} \mathbf{l}_{n,k}^{\mathrm{T}}\left\{\mathbf{\Psi}_{n,k} - \left(\mathbf{\Psi}_{n,k}\mathbf{D}_{n,k}^{\mathrm{T}}\right)\left(\mathbf{D}_{n,k}\mathbf{\Psi}_{n,k}\mathbf{D}_{n,k}^{\mathrm{T}}\right)^{-1}\left(\mathbf{D}_{n,k}\mathbf{\Psi}_{n,k}\right)\right\}\mathbf{l}_{n,k}/c^2\,, & \text{LOS} \\ 0\,, & \text{NLOS} \end{cases} \tag{14}$$

the agent, the properties of the received waveforms, the array geometry, and the array orientation.

The SPEB and SOEB can be obtained from $\mathbf{J}_{\rm e}(\mathbf{p})$ and $J_{\rm e}(\varphi)$ through (15) and (16 ), respectively. Although not apparent in (16), it is shown in [6] that $\mathcal{P}(\varphi)$ does not depend on the specific reference point. This is because different reference points only introduce different translations, but not rotations. In contrary, $\mathbf{J}_{\rm e}(\mathbf{p})$ depends on the specific reference point $\mathbf{p}$ since both $h_{n,k}$ and $\mathbf{q}$ depend on $\mathbf{p}$. The SPEB for any reference point $\mathbf{p}$ is given by [6]

$$\mathcal{P}(\mathbf{p}) = \mathcal{P}(\mathbf{p}^*) + \mathcal{P}(\varphi) \cdot \|\mathbf{p} - \mathbf{p}^*\|^2 . \tag{19}$$

This implies that the SPEB of $\mathbf{p}$ is equal to that of the orientation center $\mathbf{p}^*$ plus the orientation-induced position error. The latter is proportional to the squared distance from $\mathbf{p}$ to $\mathbf{p}^*$ and the SOEB.

The EFIM $\mathbf{J}_{\rm e}(\mathbf{p})$ in (15) depends only on the ranging information between each pair of anchors and antennas (through $\lambda_{n,k}$'s and $\phi_{n,k}$'s), and the array geometry (through $h_{n,k}$'s). Thus, AOA measurements obtained at the antenna array does not further increase the position accuracy. Intuitively, AOA is obtained indirectly by the antenna array through TOA measurements, whereas the TOA information has already been fully utilized for localization by individual antennas.

### C. EFIM in Far-Field Scenarios

We now investigate localization in far-field scenarios, where the antennas in the array are closely located such that the received waveforms from each anchor experience propagation channels with the same statistics. In such cases, we have $\phi_{n,k} = \phi_k$, $\lambda_{n,k} = \lambda_k$, and $\mathbf{q}_{n,k} = \mathbf{q}_k$ for all $n$.

Take the array center $\mathbf{p}_0$ as the reference point, and we have

$$\sum_{n\in\mathcal{N}_{\rm a}} h_{n,k} = \frac{d}{d\varphi}\Big[ \sum_{n\in\mathcal{N}_{\rm a}} \Delta x_n(\mathbf{p}_0,\varphi)\, \cos\phi_{n,k} + \sum_{n\in\mathcal{N}_{\rm a}} \Delta y_n(\mathbf{p}_0,\varphi)\, \sin\phi_{n,k}\Big] = 0 ,$$

and the corresponding

$$\mathbf{q} = \sum_{n\in\mathcal{N}_{\rm a}}\sum_{k\in\mathcal{N}_{\rm b}} \lambda_k h_{n,k}\, \mathbf{q}_k = \sum_{k\in\mathcal{N}_{\rm b}} \left(\sum_{n\in\mathcal{N}_{\rm a}} h_{n,k}\right) \lambda_k\, \mathbf{q}_k = 0 ,$$

which implies $\mathbf{p}_0 = \mathbf{p}^*$. Hence, the array center becomes the orientation center in far-field scenarios and always achieves the minimum SPEB. Moreover, the array center is a well-suited choice for the reference point since it can be determined from the array geometry alone, without requiring the received waveforms or the knowledge of the agent-anchor topology.

Following an analysis similar to Section III-A together with the fact that the array center is the orientation center, we obtain the EFIM for the array center and the EFI for the orientation as

$$\mathbf{J}_{\rm e}(\mathbf{p}_0) = N_{\rm a} \sum_{k\in\mathcal{N}_{\rm b}} \lambda_k\, \mathbf{q}_k\, \mathbf{q}_k^{\rm T} , \tag{20}$$

and

$$J_{\rm e}(\varphi) = \sum_{n\in\mathcal{N}_{\rm a}}\sum_{k\in\mathcal{N}_{\rm b}} \lambda_k\, \bar{h}_{n,k}^2 , \tag{21}$$

where $\sum_{k\in\mathcal{N}_{\rm b}} \lambda_k\, \mathbf{q}_k\, \mathbf{q}_k^{\rm T}$ is the EFIM corresponding to a single antenna, and $\bar{h}_{n,k}$ is the function $h_{n,k}$ evaluated at $\mathbf{p}_0$. Note that in such scenarios, the localization performance of an $N_{\rm a}$-antenna array is equivalent to that of a single antenna with $N_{\rm a}$ measurements, regardless of the array geometry.

We now illustrate an application of (21) for AOA estimation using wideband antenna arrays. Consider a position-aware localization problem in a far-field scenario. Since $\phi_k$ is known, estimation of the AOA from anchor $k$ to the array, i.e., $\widetilde{\phi}_k \triangleq \phi_k - \varphi$, is equivalent to the estimation of the array orientation. The contribution of anchor $k$ in (21) becomes exactly the EFI for the AOA from anchor $k$ to the array, i.e.,

$$J_{\rm e}(\widetilde{\phi}_k) = \lambda_k \sum_{n\in\mathcal{N}_{\rm a}} \bar{h}_{n,k}^2 , \tag{22}$$

from which the error bound of AOA estimation can be obtained.

## IV. Discussion

In this section, we will investigate the contribution of a priori knowledge to the localization accuracy. The a priori knowledge includes that of channel parameters, agent's position and orientation, and multipath geometry. We will also exemplify our results using two specific array geometries.

### A. Contribution from A Priori Knowledge

We consider a scenario in which the channel parameter vectors $\boldsymbol{\kappa}_{n,k}$ are independent for different $n$'s and $k$'s. The independence assumption serves as a reasonable approximation of many realistic scenarios, especially near-field cases. When the different sets of channel parameters are correlated, our results provide an upper bound for the EFIM since correlation in parameters decreases the Fisher information.

The joint probability density function (PDF) of random parameter vector $\boldsymbol{\theta}$ obtained from a priori knowledge can be written as[10]

$$f(\boldsymbol{\theta}) = f(\mathbf{p})\, f(\varphi) \prod_{n\in\mathcal{N}_{\rm a}} \prod_{k\in\mathcal{N}_{\rm b}} f(\boldsymbol{\kappa}_{n,k}|\mathbf{p},\varphi) , \tag{23}$$

where $f(\mathbf{p})$ and $f(\varphi)$ are the PDFs of the reference point $\mathbf{p}$ and the orientation $\varphi$ respectively, and $f(\boldsymbol{\kappa}_{n,k}|\mathbf{p},\varphi)$ is the PDF of the channel parameters conditioned on $\mathbf{p}$ and $\varphi$.

*1) Localization with A Priori Channel Knowledge:* When a priori channel knowledge is available, the likelihood function of the random vectors $\mathbf{r}$ and $\boldsymbol{\theta}$ can be written as

$$f(\mathbf{r},\boldsymbol{\theta}) = \prod_{n\in\mathcal{N}_{\rm a}} \prod_{k\in\mathcal{N}_{\rm b}} f(\mathbf{r}_{n,k}|\boldsymbol{\theta}) f(\boldsymbol{\kappa}_{n,k}|\mathbf{p},\varphi),$$

where $f(\mathbf{r}_{n,k}|\boldsymbol{\theta})$ is given by (8). We then have the FIM for $\boldsymbol{\theta}$ as follows

$$\mathbf{J}_{\boldsymbol{\theta}} = \mathbf{F}_{\mathbf{r},\boldsymbol{\theta}}(\mathbf{r},\boldsymbol{\theta}\,;\boldsymbol{\theta},\boldsymbol{\theta}) \triangleq \mathbf{J}_{\rm w} + \mathbf{J}_{\rm p} ,$$

where $\mathbf{J}_{\rm w} \triangleq \mathbf{F}_{\mathbf{r},\boldsymbol{\theta}}(\mathbf{r}|\boldsymbol{\theta}\,;\boldsymbol{\theta},\boldsymbol{\theta})$ and $\mathbf{J}_{\rm p} \triangleq \mathbf{F}_{\boldsymbol{\theta}}(\boldsymbol{\theta}\,;\boldsymbol{\theta},\boldsymbol{\theta})$ are the FIMs corresponding to observation and a priori knowledge, respectively.

[10]This is a general expression of a priori PDF, where all parameters are assumed random. If some parameters are deterministic, the corresponding $f(\cdot)$'s are eliminated from (23), and we do not take expectation over these parameters in (5) as well.

The FIM $\mathbf{J}_{\rm w}$ can be obtained by taking expectation of $\mathbf{J}_{\boldsymbol{\theta}}$ in (10) over the parameter vector $\boldsymbol{\theta}$, and we will adopt notation $\bar{\boldsymbol{\Psi}}_{n,k} \triangleq \mathbb{E}_{\boldsymbol{\theta}}\{\boldsymbol{\Psi}_{n,k}\}$.

We then proceed to derive $\mathbf{J}_{\rm p}$. It has been shown that $f(\boldsymbol{\kappa}_{n,k}|\mathbf{p},\varphi) = f(\boldsymbol{\kappa}_{n,k}|d_{n,k})$ [6], where $d_{n,k} = \|\tilde{\mathbf{p}}_n - \mathbf{p}_k\|$. Define

$$\tilde{\Xi}^{n,k}_{\mathbf{p},\mathbf{p}} \triangleq \mathbf{F}_{\boldsymbol{\theta}}(\boldsymbol{\kappa}_{n,k}|d_{n,k}\,;d_{n,k},d_{n,k})\,,$$
$$\tilde{\boldsymbol{\Xi}}^{n,k}_{\mathbf{p},\boldsymbol{\kappa}} \triangleq \mathbf{F}_{\boldsymbol{\theta}}(\boldsymbol{\kappa}_{n,k}|d_{n,k}\,;d_{n,k},\boldsymbol{\kappa}_{n,k})\,,$$

and

$$\boldsymbol{\Xi}^{n,k}_{\boldsymbol{\kappa},\boldsymbol{\kappa}} \triangleq \mathbf{F}_{\boldsymbol{\theta}}(\boldsymbol{\kappa}_{n,k}|d_{n,k}\,;\boldsymbol{\kappa}_{n,k},\boldsymbol{\kappa}_{n,k})\,.$$

After some algebra, we can obtain the FIM from the a priori knowledge as (24), shown at the bottom of this page, where $\boldsymbol{\Xi}^{n,k}_{\mathbf{p},\mathbf{p}} = \mathbf{q}_{n,k}\,\tilde{\Xi}^{n,k}_{\mathbf{p},\mathbf{p}}\,\mathbf{q}_{n,k}^{\rm T}$, $\boldsymbol{\Xi}^{n,k}_{\mathbf{p},\varphi} = \mathbf{q}_{n,k}\,\tilde{\Xi}^{n,k}_{\mathbf{p},\mathbf{p}}\,h_{n,k}$, $\Xi^{n,k}_{\varphi,\varphi} = h^2_{n,k}\,\tilde{\Xi}^{n,k}_{\mathbf{p},\mathbf{p}}$,

$$\boldsymbol{\Xi}_{\mathbf{p},n} = \left[\begin{array}{cccc} \boldsymbol{\Xi}^{n,1}_{\mathbf{p},\boldsymbol{\kappa}} & \boldsymbol{\Xi}^{n,2}_{\mathbf{p},\boldsymbol{\kappa}} & \cdots & \boldsymbol{\Xi}^{n,N_{\rm b}}_{\mathbf{p},\boldsymbol{\kappa}} \end{array}\right],$$
$$\boldsymbol{\Xi}_{\varphi,n} = \left[\begin{array}{cccc} \boldsymbol{\Xi}^{n,1}_{\varphi,\boldsymbol{\kappa}} & \boldsymbol{\Xi}^{n,2}_{\varphi,\boldsymbol{\kappa}} & \cdots & \boldsymbol{\Xi}^{n,N_{\rm b}}_{\varphi,\boldsymbol{\kappa}} \end{array}\right],$$

and

$$\boldsymbol{\Xi}_n = \mathrm{diag}\left\{\boldsymbol{\Xi}^{n,1}_{\boldsymbol{\kappa},\boldsymbol{\kappa}}, \boldsymbol{\Xi}^{n,2}_{\boldsymbol{\kappa},\boldsymbol{\kappa}}, \ldots, \boldsymbol{\Xi}^{n,N_{\rm b}}_{\boldsymbol{\kappa},\boldsymbol{\kappa}}\right\},$$

with $\boldsymbol{\Xi}^{n,k}_{\mathbf{p},\boldsymbol{\kappa}} = \mathbf{q}_{n,k}\,\tilde{\boldsymbol{\Xi}}^{n,k}_{\mathbf{p},\boldsymbol{\kappa}}$ and $\boldsymbol{\Xi}^{n,k}_{\varphi,\boldsymbol{\kappa}} = h_{n,k}\,\tilde{\boldsymbol{\Xi}}^{n,k}_{\mathbf{p},\boldsymbol{\kappa}}$.

Combining $\mathbf{J}_{\rm w}$ and $\mathbf{J}_{\rm p}$, we can then apply the notion of EFI to derive the $3\times 3$ EFIM $\mathbf{J}_{\rm e}(\mathbf{p},\varphi)$ in the same form as (13), where the RII $\lambda_{n,k}$ is now given by (25), shown at the bottom of the page. The RII in (25) accounts for the a priori channel knowledge, and as can be expected, it degenerates to (14) if the channel knowledge is unavailable.

*2) Localization with Position and Orientation Knowledge:* We next consider the case in which a priori knowledge of the agent's position and orientation is available. Note that the topology, i.e., relative positions of all the antennas in the network, changes with the agent's positions and orientations. The expression of the EFIM for this general case is very involved, and hence we give the result for far-field scenarios as they provide insights into the contribution of the a priori knowledge of the agent's position and orientation to localization.

In far-field scenarios, $\phi_{n,k}$'s are approximately the same for every possible agent's position and orientation, and so are $d_{n,k}$'s. Moreover, we approximate $\mathbf{p} = \mathbb{E}_{\mathbf{p}}\{\mathbf{p}\} = \mathbf{p}_0$. Note that for a fixed $k$, $\alpha^{(l)}_{n,k}$'s are the same for all $n$ and so are $b^{(l)}_{n,k}$'s. After some algebra, the $3\times 3$ EFIM for the array center and orientation can be written as

$$\mathbf{J}_{\rm e}(\mathbf{p}_0,\varphi) = \mathrm{diag}\Bigg\{ N_{\rm a}\sum_{k\in\mathcal{N}_{\rm b}} \bar{\lambda}_k\,\mathbf{q}_k\,\mathbf{q}_k^{\rm T} + \boldsymbol{\Xi}_{\mathbf{p}}\,, \sum_{n\in\mathcal{N}_{\rm a}}\sum_{k\in\mathcal{N}_{\rm b}} \bar{\lambda}_k\,\bar{h}^2_{n,k} + \Xi_{\varphi}\Bigg\},$$

where $\boldsymbol{\Xi}_{\mathbf{p}} \triangleq \mathbf{F}_{\mathbf{p}}(\mathbf{p}\,;\mathbf{p},\mathbf{p})$, $\Xi_{\varphi} \triangleq \mathbf{F}_{\varphi}(\varphi\,;\varphi,\varphi)$, and $\bar{h}_{n,k}$, $\bar{\lambda}_k$, and $\mathbf{q}_k$ are evaluated at $\mathbf{p}_0$. Consequently, the EFIM for the position and the EFI for the orientation are given given by

$$\mathbf{J}_{\rm e}(\mathbf{p}_0) = N_{\rm a}\sum_{k\in\mathcal{N}_{\rm b}} \bar{\lambda}_k\,\mathbf{q}_k\,\mathbf{q}_k^{\rm T} + \boldsymbol{\Xi}_{\mathbf{p}}\,,$$

and

$$J_{\rm e}(\varphi) = \sum_{n\in\mathcal{N}_{\rm a}}\sum_{k\in\mathcal{N}_{\rm b}} \bar{\lambda}_k\,\bar{h}^2_{n,k} + \Xi_{\varphi}\,,$$

where the a priori position and orientation knowledge contribute to the EFIM in the form of additive terms $\boldsymbol{\Xi}_{\mathbf{p}}$ and $\Xi_{\varphi}$.

### *B. Geometric Relationship of Multipath Propagation*

Multipath propagation refers to a phenomenon in which a signal reaches the receive antenna via multiple paths, arising from either reflecting off objects or scattering. The MPCs from reflecting can be thought of as direct paths from the virtual anchors behind the reflecting surfaces (see Fig. 2).[11] Thus, at the antenna array, the arrival times of the signal from the same virtual anchor are dependent. We refer to this as the geometric relationship of multipath propagation.[12] Such a relationship may appear to be useful for localization at first glance. This, however, is not the case when the MPCs are resolvable.

*Proposition 1:* When MPCs are resolvable, the geometric relationship of multipath propagation does not contribute to the localization accuracy.

*Proof:* See Appendix A. □

Note that signals from virtual anchors are equivalent to those from agents with no a priori position knowledge. Hence,

[11]Since wider transmission bandwidths translate to higher multipath resolution, dominant MPCs can be resolved via the use of wide bandwidth signals [16]–[20].

[12]If the reflection is not ideal, for example the wall is not flat in Fig. 2, then the corresponding MPCs at the array can be thought of as direct paths coming from different virtual anchors. In such cases, a geometric relationship among the MPCs does not exist.

$$\mathbf{J}_{\rm p} = \left[\begin{array}{ccccc} \sum_{n\in\mathcal{N}_{\rm a}}\sum_{k\in\mathcal{N}_{\rm b}} \boldsymbol{\Xi}^{n,k}_{\mathbf{p},\mathbf{p}} & \sum_{n\in\mathcal{N}_{\rm a}}\sum_{k\in\mathcal{N}_{\rm b}} \boldsymbol{\Xi}^{n,k}_{\mathbf{p},\varphi} & \boldsymbol{\Xi}_{\mathbf{p},1} & \cdots & \boldsymbol{\Xi}_{\mathbf{p},N_{\rm a}} \\ \sum_{n\in\mathcal{N}_{\rm a}}\sum_{k\in\mathcal{N}_{\rm b}} \boldsymbol{\Xi}^{n,k\,\rm T}_{\mathbf{p},\varphi} & \sum_{n\in\mathcal{N}_{\rm a}}\sum_{k\in\mathcal{N}_{\rm b}} \Xi^{n,k}_{\varphi,\varphi} & \boldsymbol{\Xi}_{\varphi,1} & \cdots & \boldsymbol{\Xi}_{\varphi,N_{\rm a}} \\ \boldsymbol{\Xi}^{\rm T}_{\mathbf{p},1} & \boldsymbol{\Xi}^{\rm T}_{\varphi,1} & \boldsymbol{\Xi}_1 & & \\ \vdots & \vdots & & \ddots & \\ \boldsymbol{\Xi}^{\rm T}_{\mathbf{p},N_{\rm a}} & \boldsymbol{\Xi}^{\rm T}_{\varphi,N_{\rm a}} & & & \boldsymbol{\Xi}_{N_{\rm a}} \end{array}\right] \tag{24}$$

$$\lambda_{n,k} = \frac{1}{c^2}\left\{\mathbf{l}_{n,k}^{\rm T}\bar{\boldsymbol{\Psi}}_{n,k}\mathbf{l}_{n,k} + c^2\tilde{\Xi}^{n,k}_{\mathbf{p},\mathbf{p}} - \left(\mathbf{l}_{n,k}^{\rm T}\bar{\boldsymbol{\Psi}}_{n,k} + c^2\boldsymbol{\Xi}^{n,k}_{\boldsymbol{\kappa},\boldsymbol{\kappa}}\right)\left(\bar{\boldsymbol{\Psi}}_{n,k} + c^2\boldsymbol{\Xi}_{n,k}\right)^{-1}\left(\mathbf{l}_{n,k}^{\rm T}\bar{\boldsymbol{\Psi}}_{n,k} + c^2\boldsymbol{\Xi}^{n,k}_{\boldsymbol{\kappa},\boldsymbol{\kappa}}\right)^{\rm T}\right\} \tag{25}$$

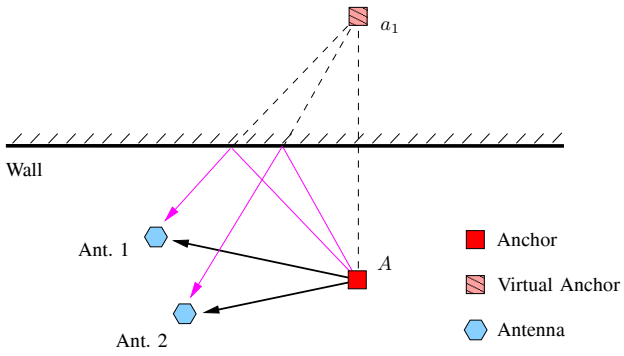


Fig. 2. Multipath geometry: MPCs come from reflecting off objects, and these paths can be considered as direct paths from virtual anchors ($a_1$ of anchor $A$).

Proposition 1 implies that cooperation with such agents does not increase the localization accuracy of the antenna array. This seems contradictory to the results in [5], [9]–[11], which show that cooperation can significantly improve localization. The discrepancy is due to the fact that the relative positions of the antennas in the array are known, unlike those of the agents in cooperative localization, and hence the estimates of the antennas' positions cannot be further improved by virtual anchors.

### C. Examples: Uniform Linear and Circular Array

The results in this paper are valid for arbitrary array geometries. We now illustrate these results for two commonly used arrays, i.e., the uniform linear array (ULA) and the uniform circular array (UCA), in far-field scenarios. Without loss of generality, we consider the array center as the reference point, and the position of each antenna in the array can be represented in terms of the array center $\mathbf{p}_0$ and the orientation $\varphi$.

- Uniform linear array:

$$\tilde{\mathbf{p}}_n = \mathbf{p}_0 + \Delta \cdot \left(n - \frac{N_\mathrm{a}+1}{2}\right) \begin{bmatrix} \cos\varphi \\ \sin\varphi \end{bmatrix},$$

  where $\Delta$ is the spacing of the antennas.
- Uniform circular array:

$$\tilde{\mathbf{p}}_n = \mathbf{p}_0 + R_0 \begin{bmatrix} \cos\left(2\pi\,\frac{n-1}{N_\mathrm{a}} + \varphi\right) \\ \sin\left(2\pi\,\frac{n-1}{N_\mathrm{a}} + \varphi\right) \end{bmatrix}, \quad (26)$$

  where $R_0$ is the radius of the array.

*1) Position and Orientation:* For orientation estimation, the EFI for the orientation can be obtained using (21) as

$$J_\mathrm{e}^\mathrm{L}(\varphi) = \frac{N_\mathrm{a}(N_\mathrm{a}-1)(N_\mathrm{a}+1)}{12}\,\Delta^2 \sum_{k\in\mathcal{N}_\mathrm{b}} \lambda_k \sin^2(\phi_k - \varphi) + \Xi_\varphi\,, \quad (27)$$

for the ULA, and

$$J_\mathrm{e}^\mathrm{C}(\varphi) = \begin{cases} 2R_0^2 \sum_{k\in\mathcal{N}_\mathrm{b}} \lambda_k \sin^2(\phi_k - \varphi) + \Xi_\varphi\,, & N_\mathrm{a} = 2\,, \\ N_\mathrm{a} R_0^2/2 \sum_{k\in\mathcal{N}_\mathrm{b}} \lambda_k + \Xi_\varphi\,, & N_\mathrm{a} > 2\,, \end{cases} \quad (28)$$

for the UCA.

For position estimation, the SPEB for the array center in far-field scenarios is the same for both the ULA and the UCA, implied by (20). However, the SPEBs for other positions are usually different, depending on the orientation accuracy provided by different array geometries. For example, the SPEBs can be calculated from (19) using (27) for the ULA and (28) for the UCA.

*2) AOA Estimation:* From (22), the EFI for the AOA from anchor $k$ to the array can be written as

$$J_\mathrm{e}^\mathrm{L}(\widetilde{\phi}_k) = \frac{N_\mathrm{a}(N_\mathrm{a}-1)(N_\mathrm{a}+1)}{12}\,\Delta^2\,\lambda_k \sin^2(\widetilde{\phi}_k) + \Xi_\varphi\,, \quad (29)$$

for the ULA, and

$$J_\mathrm{e}^\mathrm{C}(\widetilde{\phi}_k) = \begin{cases} 2R_0^2\,\lambda_k\,\sin^2(\widetilde{\phi}_k) + \Xi_\varphi\,, & N_\mathrm{a} = 2\,, \\ N_\mathrm{a} R_0^2/2\,\lambda_k + \Xi_\varphi\,, & N_\mathrm{a} > 2\,, \end{cases} \quad (30)$$

for the UCA.

Note that $J_\mathrm{e}^\mathrm{L}(\widetilde{\phi}_k)$ in (29) agrees with $J_\mathrm{e}^\mathrm{C}(\widetilde{\phi}_k)$ in (30) when $N_\mathrm{a} = 2$, as it should, since the two array geometries coincide in this case. When $N_\mathrm{a} > 2$, $J_\mathrm{e}^\mathrm{L}(\widetilde{\phi}_k)$ is highly dependent on the specific AOA, while the performance of the UCA is independent of the AOA. For a fair comparison, we consider an example with the same array size, i.e., $R_0 = (N_\mathrm{a}-1)\,\Delta/2$. If a priori orientation knowledge is unavailable, i.e., $\Xi_\varphi = 0$, then the ratio of EFIs is

$$\frac{J_\mathrm{e}^\mathrm{L}(\widetilde{\phi}_k)}{J_\mathrm{e}^\mathrm{C}(\widetilde{\phi}_k)} = \begin{cases} 1\,, & N_\mathrm{a} = 2\,, \\ \frac{2\,(N_\mathrm{a}+1)\sin^2(\widetilde{\phi}_k)}{3\,(N_\mathrm{a}-1)}\,, & N_\mathrm{a} > 2\,. \end{cases} \quad (31)$$

When $N_\mathrm{a} \geq 5$, the above ratio is always less than or equal to 1, implying that the UCA outperforms the ULA. When $N_\mathrm{a} = 3, 4$, the ratio depends on the AOA from anchor $k$ to the array, and on average,

$$\mathbb{E}_{\phi_k}\left\{\frac{J_\mathrm{e}^\mathrm{L}(\widetilde{\phi}_k)}{J_\mathrm{e}^\mathrm{C}(\widetilde{\phi}_k)}\right\} = \frac{(N_\mathrm{a}+1)}{3\,(N_\mathrm{a}-1)} < 1\,, \quad (32)$$

provided that $\phi_k$ is uniformly distributed on $[\,0, 2\pi)$. Therefore, we conclude that the UCA can provide better AOA estimates.

### D. Multiple Antennas at Anchors

The discussion above focuses on the case where each anchor is equipped with only one antenna. From the result in (15), the gain of using an antenna array at the agent mainly comes from the multiple copies of the waveform received at different antennas.[13] Hence, the localization performance using an $N_\mathrm{a}$-antenna array is equivalent to that of a single antenna with measurements in $N_\mathrm{a}$ time slots, and the advantage of using antenna arrays lies in their ability for simultaneous measurements at the agent.

When anchors are equipped with multiple antennas, each antenna can be viewed as an individual anchor, and the agent's SPEB decreases with the number of the antennas at each anchor. If the antennas of a given anchor are closely located, multipath propagations from these "individual anchors" are highly correlated and the agent-anchor topology gives approximately the same AOA. In such cases, the antennas of a given

[13]In near-field scenarios, there may be additional gain that arises from the spatial diversity of the multiple antennas at the agent.

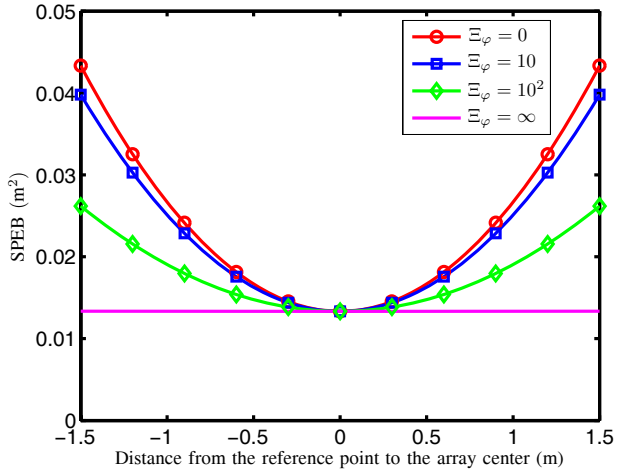


Fig. 3. SPEB as a function of the distance from the reference point to the array center for different a priori knowledge of the orientation $\Xi_\varphi$.

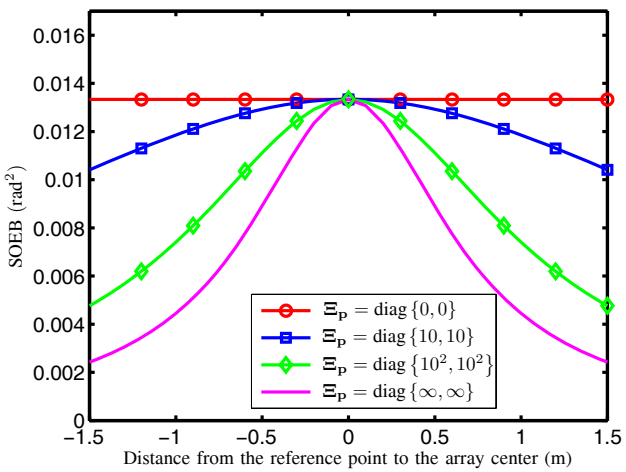


Fig. 4. SOEB as a function of the distance from the reference point to the array center for different a priori knowledge of the reference point $\mathbf{\Xi_p}$.

anchor will provide ranging information to the agent with highly correlated intensity and direction.

## V. Numerical Results

In this section, we provide several numerical examples to illustrate applications of our results.

### A. SPEB with A Priori Knowledge of Orientation

We investigate the SPEB for different reference points of a ULA when a priori knowledge of the orientation is available. The numerical results are based on a network with six equally spaced anchor nodes ($N_\mathrm{b} = 6$) located on a circle with an agent in the center. The agent is equipped with a 5-antenna array ($N_\mathrm{a} = 5$) with spacing $\Delta = 0.5\,\mathrm{m}$. In far-field scenarios, $\lambda_{n,k} = \lambda_k = 10$ and $\phi_{n,k} = \phi_k$. The SPEB as a function of different reference points along the ULA is plotted in Fig. 3 for different a priori knowledge of the orientation, $\Xi_\varphi$. First, we see that a priori knowledge of the orientation improves the localization accuracy since the SPEB decreases with increasing $\Xi_\varphi$. The curve of $\Xi_\varphi = \infty$ corresponds to orientation-aware localization, and the curve of $\Xi_\varphi = 0$ corresponds to the cases where orientation is unknown. Second, the array center has the best localization accuracy, and its SPEB does not depend on $\Xi_\varphi$, which agrees with (21). Third, the SPEB increases with both the distance from the reference point to the array center and the SOEB, as shown by (19). Fourth, the SPEB is independent of the specific reference point if $\Xi_\varphi = \infty$, and this situation is referred to as orientation-aware localization.

### B. SOEB with A Priori Knowledge of Reference Point

We now examine the SOEB for different reference points of a ULA when a priori knowledge of the reference point is available. The parameters are the same as those in Section V-A except that a priori knowledge of the reference point is available instead. The SOEB as a function of different reference points along the ULA is plotted in Fig. 4 for different a priori knowledge of the reference point, $\mathbf{\Xi_p}$. The results are counterparts of those in Fig. 3. First, a priori knowledge of the reference point improves the orientation accuracy since the SOEB decreases with increasing $\mathbf{\Xi_p}$. This agrees with both intuition and (21). Second, the array center has the worst orientation accuracy, and its SOEB does not depend on $\mathbf{\Xi_p}$. This is due to the fact that the knowledge for the array center gives no information about the array orientation. Third, the SOEB decreases as a function of the distance from the reference point to the array center if a priori knowledge of the reference point is available. Fourth, the SOEB is independent of the specific reference point if $\mathbf{\Xi_p} = \mathbf{0}$, as shown by (19).

### C. Performance Comparison of ULA and UCA

We compare the performance of the ULA and the UCA for AOA estimation as a function of the number of antennas in the array. We consider a case where the a priori knowledge of the orientation is unavailable, i.e., $\Xi_\varphi = 0$, and Fig. 5 shows the ratio of SOEBs corresponding to the UCA and the ULA for different AOA, $\tilde{\phi} \triangleq \phi - \varphi$. First, the performance of the ULA and the UCA is always the same for $N_\mathrm{a} = 2$, since they have the same array geometry in this case. Second, the ratio highly depends on $\tilde{\phi}$ for $N_\mathrm{a} = 3, 4$, while it is less than or equal to 1 for $N_\mathrm{a} \geq 5$. But the average ratio over uniform $\phi \in [0, 2\pi)$ is always less than 1, implying that the UCA outperforms the ULA. These observations were predicted by (31) and (32). Finally, the asymptotic ratio as $N_\mathrm{a} \to \infty$ is

$$\lim_{N_\mathrm{a}\to\infty} \frac{\mathcal{P}_\mathrm{C}(\tilde{\phi})}{\mathcal{P}_\mathrm{L}(\tilde{\phi})} = \lim_{N_\mathrm{a}\to\infty} \frac{J_\mathrm{e}^\mathrm{L}(\tilde{\phi})}{J_\mathrm{e}^\mathrm{C}(\tilde{\phi})} = \frac{2}{3}\sin^2(\tilde{\phi})\,.$$

## VI. Conclusion

In this paper, we consider the problem of localizing nodes using wideband antenna arrays in location-aware networks. We derived the squared position error bound (SPEB) and the squared orientation error bound (SOEB) to characterize the position and orientation accuracy. Our results reveal that both

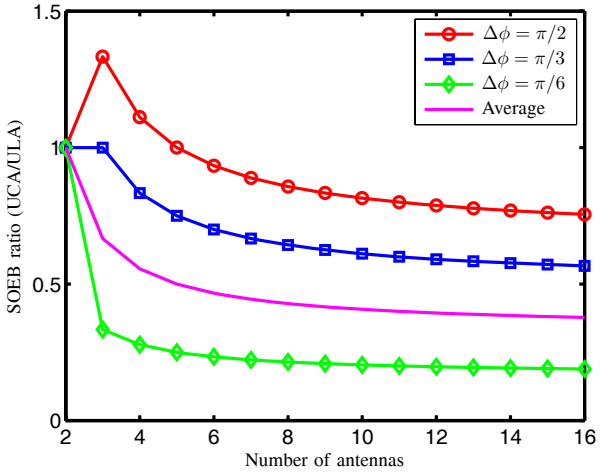


Fig. 5. Ratio of SOEBs for the ULA and UCA as a function of different number of antennas in the array. The four curves correspond to $\tilde{\phi} = \pi/6, \pi/3, \pi/2$, and average over uniform $\tilde{\phi} \in [0, 2\pi)$.

the AOA measurements obtained by antenna arrays and the geometric relationship of multipath propagation do not further improve the localization accuracy beyond that provided by TOA measurements. In the absence of a priori knowledge of the position and orientation, the SOEB is proven to be independent of the reference points, while the SPEB increases with the distance from the reference point to the orientation center, which has the minimum SPEB. In far-field scenarios, the array center becomes the orientation center, and the localization performance of an $N_{\rm a}$-antenna array is equivalent to that of a single antenna with $N_{\rm a}$ measurements. We also characterized the performance of AOA estimation using two array geometries, the UCA and ULA. The comparison showed that the UCA can provide better AOA estimates than the ULA.

## Appendix A
## Proof of Proposition 1

Consider the numbers of MPCs at the antennas coming from each anchor be the same, i.e., $L_{n,k} = L_k$ for all $n$, and when a certain MPC in the waveform at a particular antenna does not exist, its amplitude is assigned to be zero. Furthermore, we consider all the first paths to be LOS, and the amplitudes of the first paths in NLOS signals are assigned to be zero.

For each anchor $k$, there is one real anchor with known position $\mathbf{p}_k^{(1)} = \mathbf{p}_k$ and $L_k - 1$ virtual anchors with unknown position $\mathbf{p}_k^{(l)}$ $(l = 2, \ldots, L_k)$. Hence the relationship (3) becomes

$$\tau_{n,k}^{(l)} = \frac{1}{c} \left\| \mathbf{p}_k^{(l)} - \tilde{\mathbf{p}}_n \right\| ,$$

and the parameter vector $\boldsymbol{\theta}$ in (4) becomes

$$\boldsymbol{\theta} = \left[ \mathbf{p}^{\rm T} \;\; \varphi \;\; \tilde{\mathbf{p}}_1^{\rm T} \;\; \tilde{\mathbf{p}}_2^{\rm T} \;\; \cdots \;\; \tilde{\mathbf{p}}_{N_{\rm b}}^{\rm T} \;\; \boldsymbol{\alpha}_1^{\rm T} \;\; \boldsymbol{\alpha}_2^{\rm T} \;\; \cdots \;\; \boldsymbol{\alpha}_{N_{\rm a}}^{\rm T} \right]^{\rm T},$$

where $\tilde{\mathbf{p}}_k = \left[ \mathbf{p}_k^{(2)\,\rm T} \;\; \mathbf{p}_k^{(3)\,\rm T} \;\; \cdots \;\; \mathbf{p}_k^{(L_k)\,\rm T} \right]^{\rm T}$ and $\boldsymbol{\alpha}_n = \left[ \boldsymbol{\alpha}_{n,1}^{\rm T} \;\; \boldsymbol{\alpha}_{n,2}^{\rm T} \;\; \cdots \;\; \boldsymbol{\alpha}_{n,N_{\rm b}}^{\rm T} \right]^{\rm T}$, in which $\boldsymbol{\alpha}_{n,k} = \left[ \alpha_{n,k}^{(1)} \;\; \alpha_{n,k}^{(2)} \;\; \cdots \;\; \alpha_{n,k}^{(L_k)} \right]^{\rm T}$.

When MPCs are resolvable, it can be shown that

$$\mathbf{F}_{\mathbf{r}}(\mathbf{r}|\boldsymbol{\theta}\,; \alpha_{n,k}^{(i)}, \tau_{n,k}^{(j)}) = 0\,, \qquad \forall\, i\,, j\,,$$
$$\mathbf{F}_{\mathbf{r}}(\mathbf{r}|\boldsymbol{\theta}\,; \tau_{n,k}^{(i)}, \tau_{n,k}^{(j)}) = 0\,, \qquad \forall\, i \neq j\,,$$

and

$$\mathbf{F}_{\mathbf{r}}(\mathbf{r}|\boldsymbol{\theta}\,; \alpha_{n,k}^{(i)}, \alpha_{n,k}^{(j)}) = 0\,, \qquad \forall\, i \neq j\,.$$

We also define

$$\lambda_{n,k}^{(l)} \triangleq \frac{1}{c^2}\, \mathbf{F}_{\mathbf{r}}(\mathbf{r}|\boldsymbol{\theta}\,; \tau_{n,k}^{(l)}, \tau_{n,k}^{(l)}) = \frac{8\pi^2\beta^2}{c^2}\, \mathsf{SNR}_{n,k}^{(l)}\,,$$

where $\beta$ and $\mathsf{SNR}_{n,k}^{(l)}$ are given in (12).

The FIM for the parameter $\boldsymbol{\theta}$ can be expressed as

$$\mathbf{J}_{\boldsymbol{\theta}} = \begin{bmatrix} \mathbf{A} & \mathbf{B} & \mathbf{0} \\ \mathbf{B}^{\rm T} & \mathbf{C} & \mathbf{0} \\ \mathbf{0} & \mathbf{0} & \mathbf{D} \end{bmatrix}, \tag{33}$$

where

$$\mathbf{A} \triangleq \mathbf{F}_{\mathbf{r}}(\mathbf{r}|\boldsymbol{\theta}\,; \{\mathbf{p}^{\rm T}, \varphi\}, \{\mathbf{p}^{\rm T}, \varphi\})\,,$$
$$\mathbf{B} \triangleq \mathbf{F}_{\mathbf{r}}(\mathbf{r}|\boldsymbol{\theta}\,; \{\mathbf{p}^{\rm T}, \varphi\}, \{\tilde{\mathbf{p}}_1^{\rm T}, \tilde{\mathbf{p}}_2^{\rm T}, \ldots, \tilde{\mathbf{p}}_{N_{\rm b}}^{\rm T}\})\,,$$
$$\mathbf{C} \triangleq \mathbf{F}_{\mathbf{r}}(\mathbf{r}|\boldsymbol{\theta}\,; \{\tilde{\mathbf{p}}_1^{\rm T}, \tilde{\mathbf{p}}_2^{\rm T}, \ldots, \tilde{\mathbf{p}}_{N_{\rm b}}^{\rm T}\}, \{\tilde{\mathbf{p}}_1^{\rm T}, \tilde{\mathbf{p}}_2^{\rm T}, \ldots, \tilde{\mathbf{p}}_{N_{\rm b}}^{\rm T}\})\,,$$

and

$$\mathbf{D} \triangleq \mathbf{F}_{\mathbf{r}}(\mathbf{r}|\boldsymbol{\theta}\,; \{\boldsymbol{\alpha}_1^{\rm T}, \boldsymbol{\alpha}_2^{\rm T}, \ldots, \boldsymbol{\alpha}_{N_{\rm b}}^{\rm T}\}, \{\boldsymbol{\alpha}_1^{\rm T}, \boldsymbol{\alpha}_2^{\rm T}, \ldots, \boldsymbol{\alpha}_{N_{\rm b}}^{\rm T}\})\,.$$

The expression of block matrices $\mathbf{A}$, $\mathbf{B}$, and $\mathbf{C}$ can be obtained, after some algebra, as follows:[14]

- Matrix $\mathbf{A}$ is given by (34), shown at the bottom of the next page, where $\phi_{n,k}^{(l)}$ is the angle from $\mathbf{p}_k^{(l)}$ to the $n$th antenna, $\mathbf{q}(\phi_{n,k}^{(l)}) = \left[ \cos(\phi_{n,k}^{(l)}) \;\; \sin(\phi_{n,k}^{(l)}) \right]^{\rm T}$, and

$$h_{n,k}^{(l)} = \frac{d}{d\varphi} \Delta x_n(\mathbf{p}, \varphi)\, \cos\phi_{n,k}^{(l)} + \frac{d}{d\varphi} \Delta y_n(\mathbf{p}, \varphi)\, \sin\phi_{n,k}^{(l)}\,;$$

- Matrix $\mathbf{B} = [\mathbf{B}_1 \;\; \mathbf{B}_2 \;\; \cdots \;\; \mathbf{B}_{N_{\rm b}}]$, where each block matrix is given by (35), shown at the bottom of the next page.
- Matrix $\mathbf{C} = \mathrm{diag}\,\{\mathbf{C}_1, \mathbf{C}_2, \ldots, \mathbf{C}_{N_{\rm b}}\}$, where each block matrix is given by[15]

$$\mathbf{C}_k = \mathrm{diag}\Bigg\{ \sum_{n \in \mathcal{N}_{\rm a}} \lambda_{n,k}^{(2)}\, \mathbf{q}(\phi_{n,k}^{(2)})\, \mathbf{q}^{\rm T}(\phi_{n,k}^{(2)})\,, \ldots, \sum_{n \in \mathcal{N}_{\rm a}} \lambda_{n,k}^{(L_k)}\, \mathbf{q}(\phi_{n,k}^{(L_k)})\, \mathbf{q}^{\rm T}(\phi_{n,k}^{(L_k)}) \Bigg\}.$$

Apply the notion of the EFI [6] to the original FIM in (33), and we have the EFIM for the position and orientation

$$\mathbf{J}_{\rm e}(\mathbf{p}, \varphi) = \mathbf{A} - \mathbf{B}\mathbf{C}^{-1}\mathbf{B}^{\rm T} = \mathbf{A} - \sum_{k \in \mathcal{N}_{\rm b}} \mathbf{B}_k \mathbf{C}_k^{-1} \mathbf{B}_k^{\rm T}\,. \tag{36}$$

[14]It will be apparent later that the exact expression for the block matrix $\mathbf{D}$ is not necessary.

[15]The diagonal structure of $\mathbf{C}$ is due to the fact that virtual anchors do not communicate with each other.

The component $\mathbf{B}_k\mathbf{C}_k^{-1}\mathbf{B}_k^{\mathrm{T}}$ is derived in (37), shown at the bottom of the page, where we have used

$$\sum_{n\in\mathcal{N}_\mathrm{a}} \lambda_{n,k}^{(l)} h_{n,k}^{(l)}\, \mathbf{q}^{\mathrm{T}}(\phi_{n,k}^{(l)}) = \left[\begin{array}{cc} \frac{d}{d\varphi}\Delta x_n(\mathbf{p},\varphi) & \frac{d}{d\varphi}\Delta y_n(\mathbf{p},\varphi) \end{array}\right] \times \sum_{n\in\mathcal{N}_\mathrm{a}} \lambda_{n,k}^{(l)}\, \mathbf{q}(\phi_{n,k}^{(l)})\, \mathbf{q}^{\mathrm{T}}(\phi_{n,k}^{(l)})\,.$$

Substituting (37) and (34) into (36), and noting that $\mathbf{A}$ and $\mathbf{B}\mathbf{C}^{-1}\mathbf{B}^{\mathrm{T}}$ differ only by terms involving $l=1$, we have (38), shown at the bottom of the page, which is equal to the EFIM of the case where environmental knowledge is not exploited.

## ACKNOWLEDGMENT

The authors would like to thank W. Suwansantisuk, W. M. Gifford, H. Wymeersch, P. Pinto, and S. Mazuelas for their valuable suggestions and careful reading of the manuscript. We would also like to thank the anonymous reviewers for their constructive comments.

## REFERENCES

[1] J. J. Spilker, Jr., "GPS signal structure and performance characteristics," *J. Institute Navigation*, vol. 25, no. 2, pp. 121-146, Summer 1978.

[2] D. B. Jourdan, D. Dardari, and M. Z. Win, "Position error bound for UWB localization in dense cluttered environments," *IEEE Trans. Aerosp. Electron. Syst.*, vol. 44, no. 2, pp. 613-628, Apr. 2008.

[3] S. Gezici, Z. Tian, G. B. Giannakis, H. Kobayashi, A. F. Molisch, H. V. Poor, and Z. Sahinoglu, "Localization via ultra-wideband radios: a look at positioning aspects for future sensor networks," *IEEE Signal Process. Mag.*, vol. 22, pp. 70-84, July 2005.

[4] Y. Shen and M. Z. Win, "Fundamental limits of wideband localization–part I: a general framework," *IEEE Trans. Inf. Theory*, vol. 56, 2010, to appear.

[5] Y. Shen, H. Wymeersch, and M. Z. Win, "Fundamental limits of wideband localization–part II: cooperative networks," *IEEE Trans. Inf. Theory*, 2009, submitted for publication.

[6] Y. Shen, "Fundamental limits of wideband localization," Master's thesis, Department of Electrical Engineering and Computer Science, Massachusetts Institute of Technology, Cambridge, MA, Feb. 2008; thesis advisor: Professor Moe Z. Win.

[7] Y. Shen and M. Z. Win, "Fundamental limits of wideband localization accuracy via Fisher information," in *Proc. IEEE Wireless Commun. Netw. Conf.*, Kowloon, Hong Kong, Mar. 2007, pp. 3046-3051.

[8] ——, "Performance of localization and orientation using wideband antenna arrays," in *Proc. IEEE Int. Conf. Ultra-Wideband (ICUWB)*, Singapore, Sept. 2007, pp. 288-293.

[9] Y. Shen, H. Wymeersch, and M. Z. Win, "Fundamental limits of wideband cooperative localization via Fisher information," in *Proc. IEEE Wireless Commun. Networking Conf.*, Kowloon, Hong Kong, Mar. 2007, pp. 3951-3955.

[10] M. Z. Win, Y. Shen, and H. Wymeersch, "On the position error bound in cooperative networks: a geometric approach," in *Proc. IEEE Int. Symp. Spread Spectrum Techniques Applications*, Bologna, Italy, Aug. 2008, pp. 637-643.

[11] H. Wymeersch, J. Lien, and M. Z. Win, "Cooperative localization in wireless networks," *Proc. IEEE*, vol. 97, no. 2, pp. 427-450, Feb. 2009, special issue on ultra-wide bandwidth (UWB) technology emerging applications.

[12] H. Wymeersch, U. Ferner, and M. Z. Win, "Cooperative Bayesian self-tracking for wireless networks," *IEEE Commun. Lett.*, vol. 12, no. 7, pp. 505-507, July 2008.

[13] D. Dardari, A. Conti, J. Lien, and M. Z. Win, "The effect of cooperation on localization systems using UWB experimental data," *EURASIP J. Appl. Signal Process.* (special issue cooperative localization wireless ad hoc sensor netw.), vol. 2008, pp. article ID 513 873, 1-11, 2008.

[14] D. Dardari, C.-C. Chong, and M. Z. Win, "Threshold-based time-of-arrival estimators in UWB dense multipath channels," *IEEE Trans. Commun.*, vol. 56, no. 8, pp. 1366-1378, Aug. 2008.

[15] D. Dardari, A. Conti, U. J. Ferner, A. Giorgetti, and M. Z. Win, "Ranging with ultrawide bandwidth signals in multipath environments," *Proc. IEEE*, vol. 97, no. 2, pp. 404-426, Feb. 2009, special issue on ultra-wide bandwidth (UWB) technology emerging applications.

[16] M. Z. Win and R. A. Scholtz, "Impulse radio: how it works," *IEEE Commun. Lett.*, vol. 2, no. 2, pp. 36-38, Feb. 1998.

[17] ——, "Ultra-wide bandwidth time-hopping spread-spectrum impulse radio for wireless multiple-access communications," *IEEE Trans. Commun.*, vol. 48, no. 4, pp. 679-691, Apr. 2000.

[18] ——, "Characterization of ultra-wide bandwidth wireless indoor communications channel: a communication theoretic view," *IEEE J. Sel. Areas Commun.*, vol. 20, no. 9, pp. 1613-1627, Dec. 2002.

[19] A. F. Molisch, D. Cassioli, C.-C. Chong, S. Emami, A. Fort, B. Kannan, J. Karedal, J. Kunisch, H. Schantz, K. Siwiak, and M. Z. Win, "A comprehensive standardized model for ultrawideband propagation channels," *IEEE Trans. Antennas Propag.*, vol. 54, no. 11, pp. 3151-3166, Nov. 2006, special issue on wireless commun.

[20] D. Cassioli, M. Z. Win, and A. F. Molisch, "The ultra-wide bandwidth indoor channel: from statistical model to simulations," *IEEE J. Sel. Areas Commun.*, vol. 20, no. 6, pp. 1247-1257, Aug. 2002.

$$\mathbf{A} = \sum_{n\in\mathcal{N}_\mathrm{a}} \sum_{k\in\mathcal{N}_\mathrm{b}} \sum_{l=1}^{L_k} \left[\begin{array}{cc} \lambda_{n,k}^{(l)}\, \mathbf{q}(\phi_{n,k}^{(l)})\, \mathbf{q}^{\mathrm{T}}(\phi_{n,k}^{(l)}) & \lambda_{n,k}^{(l)} h_{n,k}^{(l)}\, \mathbf{q}(\phi_{n,k}^{(l)}) \\ \lambda_{n,k}^{(l)} h_{n,k}^{(l)}\, \mathbf{q}^{\mathrm{T}}(\phi_{n,k}^{(l)}) & \lambda_{n,k}^{(l)} h_{n,k}^{(l)\,2} \end{array}\right] \tag{34}$$

$$\mathbf{B}_k = \left[\begin{array}{ccc} \sum_{n\in\mathcal{N}_\mathrm{a}} \lambda_{n,k}^{(2)}\, \mathbf{q}(\phi_{n,k}^{(2)})\, \mathbf{q}^{\mathrm{T}}(\phi_{n,k}^{(2)}) & \cdots & \sum_{n\in\mathcal{N}_\mathrm{a}} \lambda_{n,k}^{(L_k)}\, \mathbf{q}(\phi_{n,k}^{(L_k)})\, \mathbf{q}^{\mathrm{T}}(\phi_{n,k}^{(L_k)}) \\ \sum_{n\in\mathcal{N}_\mathrm{a}} \lambda_{n,k}^{(2)}\, h_{n,k}^{(2)}\, \mathbf{q}^{\mathrm{T}}(\phi_{n,k}^{(2)}) & \cdots & \sum_{n\in\mathcal{N}_\mathrm{a}} \lambda_{n,k}^{(L_k)}\, h_{n,k}^{(L_k)}\, \mathbf{q}^{\mathrm{T}}(\phi_{n,k}^{(L_k)}) \end{array}\right] \tag{35}$$

$$\begin{aligned} \mathbf{B}_k\, \mathbf{C}_k^{-1}\, \mathbf{B}_k^{\mathrm{T}} &= \sum_{l=2}^{L_k} \left[\begin{array}{c} \sum_{n\in\mathcal{N}_\mathrm{a}} \lambda_{n,k}^{(l)}\, \mathbf{q}(\phi_{n,k}^{(l)})\, \mathbf{q}^{\mathrm{T}}(\phi_{n,k}^{(l)}) \\ \sum_{n\in\mathcal{N}_\mathrm{a}} \lambda_{n,k}^{(l)}\, h_{n,k}^{(l)}\, \mathbf{q}^{\mathrm{T}}(\phi_{n,k}^{(l)}) \end{array}\right] \left(\sum_{n\in\mathcal{N}_\mathrm{a}} \lambda_{n,k}^{(l)}\, \mathbf{q}(\phi_{n,k}^{(l)})\, \mathbf{q}^{\mathrm{T}}(\phi_{n,k}^{(l)})\right)^{-1} \left[\begin{array}{c} \sum_{n\in\mathcal{N}_\mathrm{a}} \lambda_{n,k}^{(l)}\, \mathbf{q}(\phi_{n,k}^{(l)})\, \mathbf{q}^{\mathrm{T}}(\phi_{n,k}^{(l)}) \\ \sum_{n\in\mathcal{N}_\mathrm{a}} \lambda_{n,k}^{(l)}\, h_{n,k}^{(l)}\, \mathbf{q}^{\mathrm{T}}(\phi_{n,k}^{(l)}) \end{array}\right]^{\mathrm{T}} \\ &= \sum_{l=2}^{L_k} \sum_{n\in\mathcal{N}_\mathrm{a}} \left[\begin{array}{cc} \lambda_{n,k}^{(l)}\, \mathbf{q}(\phi_{n,k}^{(l)})\, \mathbf{q}^{\mathrm{T}}(\phi_{n,k}^{(l)}) & \lambda_{n,k}^{(l)} h_{n,k}^{(l)}\, \mathbf{q}(\phi_{n,k}^{(l)}) \\ \lambda_{n,k}^{(l)} h_{n,k}^{(l)}\, \mathbf{q}^{\mathrm{T}}(\phi_{n,k}^{(l)}) & \lambda_{n,k}^{(l)} h_{n,k}^{(l)\,2} \end{array}\right] \end{aligned} \tag{37}$$

$$\mathbf{J}_\mathrm{e}(\mathbf{p},\varphi) = \sum_{n\in\mathcal{N}_\mathrm{a}} \sum_{k\in\mathcal{N}_\mathrm{b}} \left[\begin{array}{cc} \lambda_{n,k}^{(1)}\, \mathbf{q}(\phi_{n,k}^{(1)})\, \mathbf{q}^{\mathrm{T}}(\phi_{n,k}^{(1)}) & \lambda_{n,k}^{(1)}\, h_{n,k}^{(1)}\, \mathbf{q}(\phi_{n,k}^{(1)}) \\ \lambda_{n,k}^{(1)}\, h_{n,k}^{(1)}\, \mathbf{q}^{\mathrm{T}}(\phi_{n,k}^{(1)}) & \lambda_{n,k}^{(1)}\, h_{n,k}^{(1)\,2} \end{array}\right] \tag{38}$$

[21] A. Ridolfi and M. Z. Win, "Ultrawide bandwidth signals as shot-noise: a unifying approach," *IEEE J. Sel. Areas Commun.*, vol. 24, no. 4, pp. 899-905, Apr. 2006.
[22] W. Suwansantisuk and M. Z. Win, "Multipath aided rapid acquisition: optimal search strategies," *IEEE Trans. Inf. Theory*, vol. 53, no. 1, pp. 174-193, Jan. 2007.
[23] J.-Y. Lee and R. A. Scholtz, "Ranging in a dense multipath environment using an UWB radio link," *IEEE J. Sel. Areas Commun.*, vol. 20, no. 9, pp. 1677-1683, Dec. 2002.
[24] B. Van Veen and K. Buckley, "Beamforming: a versatile approach to spatial filtering," *IEEE Signal Process. Mag.*, vol. 5, no. 2, pp. 4-24, 1988.
[25] H. Krim and M. Viberg, "Two decades of array signal processing research: the parametric approach," *IEEE Signal Process. Mag.*, vol. 13, no. 4, pp. 67-94, 1996.
[26] R. Engelbrecht, "Passive source localization from spatially correlated angle-of-arrival data," *IEEE Trans. Signal Process.*, vol. 31, no. 4, pp. 842-846, 1983.
[27] C.-C. Chong, C.-M. Tan, D. I. Laurenson, S. McLaughlin, M. A. Beach, and A. R. Nix, "A new statistical wideband spatio-temporal channel model for 5-GHz band WLAN systems," *IEEE J. Sel. Areas Commun.*, vol. 21, no. 2, pp. 139-150, Feb. 2003.
[28] A. F. Molisch, *Wireless Communications*, 1st ed. Piscataway, NJ: IEEE Press, J. Wiley and Sons, 2005.
[29] P. Deng and P. Fan, "An AOA assisted TOA positioning system," in *Proc. Int. Conf. Commun. Technol.*, vol. 2, Beijing, China, 2000, pp. 1501-1504.
[30] Y. Qi, H. Kobayashi, and H. Suda, "Analysis of wireless geolocation in a non-line-of-sight environment," *IEEE Trans. Wireless Commun.*, vol. 5, no. 3, pp. 672-681, 2006.
[31] A. Mallat, J. Louveaux, and L. Vandendorpe, "UWB based positioning in multipath channels: CRBs for AOA and for hybrid TOA-AOA based methods," in *Proc. IEEE Int. Conf. Commun.*, Glasgow, UK, June 2007, pp. 5775-5780.
[32] L. Cong and W. Zhuang, "Hybrid TDOA/AOA mobile user location for wideband CDMA cellular systems," *IEEE Trans. Wireless Commun.*, vol. 1, no. 3, pp. 439-447, 2002.
[33] H. L. Van Trees, *Detection, Estimation and Modulation Theory*. New York: Wiley, 1968, vol. 1.
[34] H. V. Poor, *An Introduction to Signal Detection and Estimation*, 2nd ed. New York: Springer-Verlag, 1994.
[35] I. Reuven and H. Messer, "A Barankin-type lower bound on the estimation error of a hybrid parameter vector," *IEEE Trans. Inf. Theory*, vol. 43, no. 3, pp. 1084-1093, May 1997.

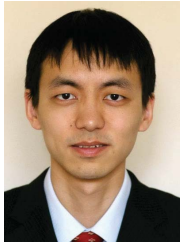

**Yuan Shen** (S'05) received his B.S. degree (with highest honor) from Tsinghua University, China, in 2005, and S.M. degree from the Massachusetts Institute of Technology (MIT) in 2008, both in electrical engineering. Since 2005, Yuan Shen has been with the Laboratory for Information and Decision Systems (LIDS) at MIT, where he is now a Ph.D. candidate. His research interests include communication theory, information theory, and statistical signal processing. His current research focuses on wideband localization, cooperative networks, and ultra-wide bandwidth communications.

He has served as a Technical Program Committee (TPC) member for the IEEE Wireless Communications & Networking Conference (WCNC) in 2009. He received the Ernst A. Guillemin Thesis Award (first place) for the best S.M. thesis from the Department of Electrical Engineering and Computer Science at MIT in 2008, the Roberto Padovani Scholarship from Qualcomm Inc. in 2008, the Best Paper Award from the IEEE Wireless Communications and Networking Conference (WCNC) in 2007, and the Walter A. Rosenblith Presidential Fellowship from MIT in 2005.

**Moe Z. Win** (S'85-M'87-SM'97-F'04) received both the Ph.D. in Electrical Engineering and M.S. in Applied Mathematics as a Presidential Fellow at the University of Southern California (USC) in 1998. He received an M.S. in Electrical Engineering from USC in 1989, and a B.S. (*magna cum laude*) in Electrical Engineering from Texas A&M University in 1987.

Dr. Win is an Associate Professor at the Massachusetts Institute of Technology (MIT). Prior to joining MIT, he was at AT&T Research Laboratories for five years and at the Jet Propulsion Laboratory for seven years. His research encompasses developing fundamental theories, designing algorithms, and conducting experimentation for a broad range of real-world problems. His current research topics include location-aware networks, time-varying channels, multiple antenna systems, ultra-wide bandwidth systems, optical transmission systems, and space communications systems.

Professor Win is an IEEE Distinguished Lecturer and elected Fellow of the IEEE, cited for "contributions to wideband wireless transmission." He was honored with the IEEE Eric E. Sumner Award (2006), an IEEE Technical Field Award for "pioneering contributions to ultra-wide band communications science and technology." Together with students and colleagues, his papers have received several awards including the IEEE Communications Society's Guglielmo Marconi Best Paper Award (2008) and the IEEE Antennas and Propagation Society's Sergei A. Schelkunoff Transactions Prize Paper Award (2003). His other recognitions include the Laurea Honoris Causa from the University of Ferrara, Italy (2008), the Technical Recognition Award of the IEEE ComSoc Radio Communications Committee (2008), Wireless Educator of the Year Award (2007), the Fulbright Foundation Senior Scholar Lecturing and Research Fellowship (2004), the U.S. Presidential Early Career Award for Scientists and Engineers (2004), the AIAA Young Aerospace Engineer of the Year (2004), and the Office of Naval Research Young Investigator Award (2003).

Professor Win has been actively involved in organizing and chairing a number of international conferences. He served as the Technical Program Chair for the IEEE Wireless Communications and Networking Conference in 2009, the IEEE Conference on Ultra Wideband in 2006, the IEEE Communication Theory Symposia of ICC-2004 and Globecom-2000, and the IEEE Conference on Ultra Wideband Systems and Technologies in 2002; Technical Program Vice-Chair for the IEEE International Conference on Communications in 2002; and the Tutorial Chair for ICC-2009 and the IEEE Semiannual International Vehicular Technology Conference in Fall 2001. He was the chair (2004-2006) and secretary (2002-2004) for the Radio Communications Committee of the IEEE Communications Society. Dr. Win is currently an Editor for IEEE TRANSACTIONS ON WIRELESS COMMUNICATIONS. He served as Area Editor for *Modulation and Signal Design* (2003-2006), Editor for *Wideband Wireless and Diversity* (2003-2006), and Editor for *Equalization and Diversity* (1998-2003), all for the IEEE TRANSACTIONS ON COMMUNICATIONS. He was Guest-Editor for the PROCEEDINGS OF THE IEEE (Special Issue on UWB Technology & Emerging Applications) in 2009 and IEEE JOURNAL ON SELECTED AREAS IN COMMUNICATIONS (Special Issue on Ultra -Wideband Radio in Multiaccess Wireless Communications) in 2002.